2 Ice Behaviour under Stress and Tools for Analysis

2.1 Reality of Ice Failure

As with other materials, testing of ice has often been carried out on small samples. This is as it should be, and the results are invaluable for our basic understanding. For some materials, for example those following a plasticity-based yield criterion, the failure surface can be modelled using the results of a single uniaxial test, usually in tension, to obtain the yield strength. In the case of ice, the situation is more complex. First, there is the question of time-dependency, so that more parameters are needed to model its response. Further complications arise, such as pressure-dependence, for which triaxial testing is needed. This is not modelled well by a pressure-dependent yield surface because of the time-independence of plasticity theory. Overriding these factors is the reality that small scale test results often bear little relation to failure stress, stress distribution, or failure mode found in field ice–structure interactions.

Reviews by Sanderson (1988) and Weeks (2010) show uniaxial compressive strengths of small scale specimens generally in the range 1–10 MPa. Small scale uniaxial tests have been reported by Sinha (1984) in an interesting programme of field testing that included first year and old ice. Strengths were in the range 1–5 MPa. Sanderson (1988) and Weeks (2010) also reviewed tests and analyses with respect to brine content, which tends to weaken the ice. They discuss tests by Wang (1979) on columnar grained ice with respect to the orientation of the c-axis, where loading parallel to the c-axis showed higher strengths than other orientations (note that the basal planes were then at right angles to the load). Tests on large ice specimens (with dimensions of 6 m × 3 m × 1.5 m thick) which were subjected to uniformly applied load at low rates showed no size effect, i.e. the strengths were similar to those found on small laboratory specimens (Chen and Lee, 1986; Wang and Poplin, 1986). These results are very useful for an understanding of ice behaviour and constituted excellent research but do not explain results obtained in the field. We know that ice failing against a vertical structure over a significant area (say of the order of 100 square meters), whether multiyear or first year ice, will impose average pressures much less than 1 MPa, and also impose high local pressures much higher than the highest uniaxial strength. There is no apparent agreement with the uniaxial strength nor any obvious way to link the two situations.

The answer to the questions just posed lies in the fact that the failure of ice acting in compression against a structure in a real field situation involves two highly significant

https://doi.org/10.1017/9781108674454.003 Published online by Cambridge University Press

localizations: first, of pressure into the localized high-pressure zones and second, the formation of a "layer" of microstructurally modified material adjacent to the structure within the high-pressure zones, not readily observed either in uniaxial testing or obtained in traditional continuum analysis. This situation is found particularly during ice crushing, a common failure mode observed in the field, even at ice speeds as low as 2.5 cm s^{-1} (Rogers et al., 1986). These zones of high pressure form and disappear in a birth-and-death process during ice crushing. The pressure distribution is far from uniform, with a parabolic shape across the high-pressure zone. This is in contrast to the uniform state of compression that would be found in a laboratory test on a cylindrical or prismatic specimen carefully machined to the desired shape. In the high-pressure zone, the peak stress is many times the uniaxial strength, with a complex triaxial state of stress, and with significant occurrence of microstructural change, especially microfracturing and dynamic recrystallization. The microstructural changes are highly time- and stress-dependent, as are the resulting stresses and strains, and they affect significantly the distribution of load and pressure on the structure applying the load. Figure 2.1 shows a representation of a typical localization, termed a "high-pressure zone" (*hpz*). These entities might be of the order of 30 cm across in field interactions of thick ice features, but are much smaller in thin ice sheets and small scale indentation. They occur at irregular intervals across the failure plane in ship– or structure–ice interaction, as illustrated in Figure 2.2, except at very low interaction speeds where creep processes predominate. Their formation is closely linked to fracture processes, which are not observed in uniformly loaded laboratory specimens. Fracture aspects still need considerable study to enable one to understand why the

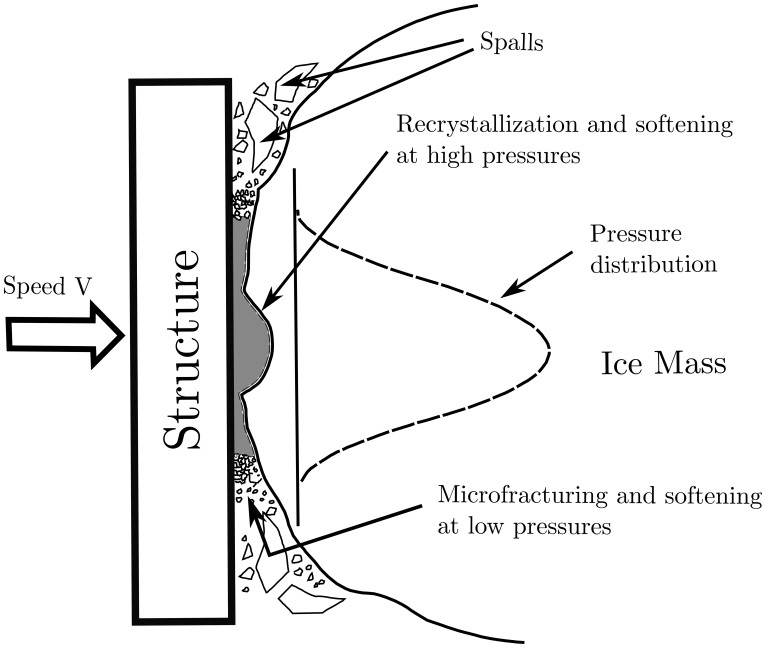

Figure 2.1 Schematic of a high-pressure zone (*hpz*). Peak pressures can be 70 MPa or higher.

https://doi.org/10.1017/9781108674454.003 Published online by Cambridge University Press

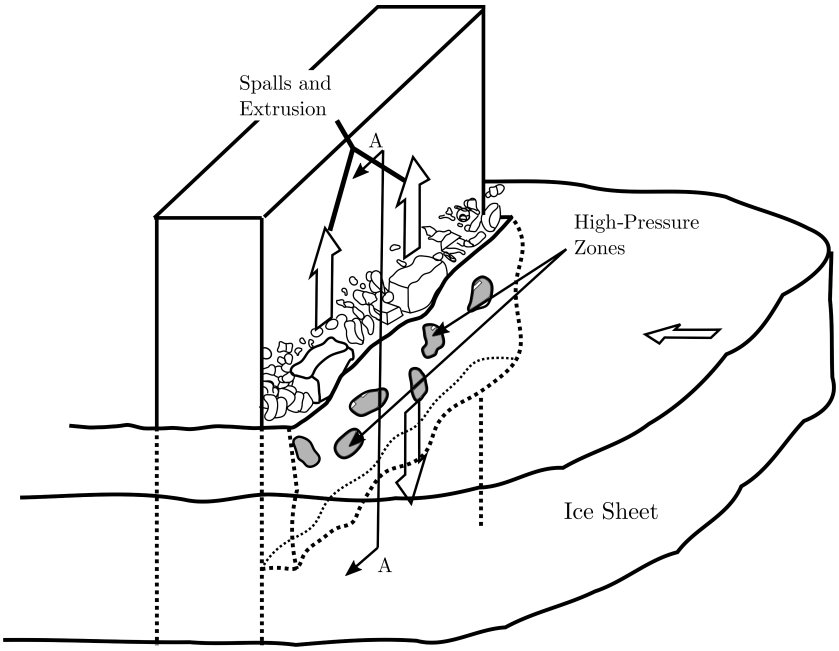

Figure 2.2 Schematic of formation of *hpz*s in interaction of structure with an ice sheet (Jordaan, 2001). With permission from Elsevier.

interaction area consisting of high-pressure zones constitutes only about 10% of the global area.

We shall analyse field data with regard to the forces imposed by *hpz*s in Part I of this work and discuss their formation and behaviour in some detail in Part II. Their existence should be borne in mind while reading the material to follow.

2.2 Creep, Fracture, Strength and Damage: Ice Crushing

Our main focus is the study of ice and its interaction with offshore structures and vessels. The emphasis is on thick ice features, multiyear ice or icebergs. Whether interacting with a ship or a structure, the ice will generally exhibit crushing failure. This rather unique failure mode was outlined in the preceding section and will be detailed throughout this work. It involves creep, fracture and changes to the ice microstructure. Ice deformation shows an extreme time-dependency. Such viscoelastic movements can relieve stress, yet ice is very brittle. The response of ice to stress depends strongly on the rate of loading and the stress level achieved. Creep is the time-dependent increase in the deformation of a material under stress. A concrete beam or slab will deform with time, occasionally resulting in unwanted deflections. Marble slabs have been known to deform considerably over time. Materials that creep include wood, many metals, steel at high temperatures, concrete, rocks, plastics, human tissues and ice. Materials at high values of homologous temperature are especially prone to creep, and ice is no

https://doi.org/10.1017/9781108674454.003 Published online by Cambridge University Press

exception. A specimen of ice loaded at constant stress will deform elastically and then over time deform by an amount that may be many times the elastic deformation. Under the compressive states of stress found in field observations of ice–structure interaction, the strain rate may be further increased by many orders of magnitude, which certainly occurs within *hpz*s.

The other dominant aspect of ice behaviour is fracture. The fracture toughness of ice is very small in value, one of the lowest values of materials on Earth. The formation of cracks will also involve time-dependent strains in the material, and as a result energy is consumed in viscoelastic deformation around the crack tip. This occurs in ice–structure interaction leading to time-dependent fracture, adding to the difficulty of analysis. A phenomenon related to this is "damage", in which the stress state and its history cause microstructural changes in the material, altering its mechanical behaviour. This area of research has been referred to as "damage mechanics", since in industrial applications, the effect on the performance of the material, e.g. steel, under stress, is of importance. In analysing a material such as ice, formed in nature, the word "damage" is rather inappropriate, but we retain it as the area of mechanics required is "damage theory" or "damage mechanics". The combination of time-dependency and brittleness makes ice a very interesting and challenging material to study, and may serve as a model for studies of other materials such as rocks and geophysical materials.

At low loading rates, ice under uniaxial compression deforms as a nonlinear viscoelastic material; at higher rates it experiences microcracking and microstructural change and at even higher rates fracture processes intervene. Uniaxial compressive strengths are typically in the range 1–10 MPa, depending on the loading rate, brine volume and other factors. Sanderson (1988) and Weeks (2010) have given good descriptions of the influencing factors. Tensile failure typically occurs at about 1 MPa. These, and other small-scale values obtained in the laboratory (or in the field), have, as noted in the preceding section, little relation to design pressures. A typical global pressure on a large structure (as measured say on the Molikpaq) might be considerably less than 1 MPa. Local pressures vary depending on the area, from say 70 MPa on areas the size of 1 cm^2 to perhaps 4–5 MPa on an area of 1 m^2. As noted in the preceding section, it is not possible to obtain such values from the measurements on uniaxial specimens; nor is it possible to deduce them from measured fracture toughness values.

During indentation and during ice–structure interaction, "crushing" failure occurs. As noted in Section 2.1, this is a special process involving fracture and consequent localization of pressure. In fact, the term "ice crushing" used to describe compressive failure of ice covers a multitude of phenomena: fractures occur in the form of flakes and spalls and many particles of crushed ice are ejected. A special process occurs under certain conditions, in which very small particles are ejected, often accompanied by larger flakes associated with spalling. The texture of the small particles is creamy and has been likened to toothpaste; such situations occur under certain conditions of interaction rate and temperature, and are associated with dynamic ice–structure interaction. The *hpz*s occuring during indentation have been found in medium scale

https://doi.org/10.1017/9781108674454.003 Published online by Cambridge University Press

tests conducted up to 3 m^2 in area but are also found in small scale indentation tests (with indentors generally 20 to 40 mm in diameter) making appropriate adjustments to the speed of indentation, as will be described in Section 8.6. It must be emphasized that the microstructural changes, when analysed in the context of the associated multiaxial state of stress and confinement, lead to profoundly altered mechanical response and behaviour, which cannot be ignored in the mechanics of ice response.

Strong analogies to the observations as summarized in the preceding paragraph can be found in the geophysical literature. Features that have a strong similarity to those just described are commonly observed. In rocks found near fault zones, cataclasis involves brittle fracture of mineral grains. This would correspond to the microfractured zones near the edges of the high-pressure zones in ice, noted in the preceding paragraph. Mylonites, on the other hand, involve reduction of grain size by a process of dynamic recrystallization, as in the centre of the high-pressure zones in ice. Sibson (1977) discusses these processes in detail. Many materials show time-dependent behaviour and also degrade with time. Concrete, ceramics, polymers and metals exhibit elasticity as well as time-dependent response to stress, and these materials may also exhibit microstructural change and microfracturing under stress, which often result in significant changes to the stress–strain behaviour, and in the case of ice, totally transform the response. All of the behaviours discussed—creep, fracture and damage—are present in ice and geophysical materials under stress. In the case of ice, these phenomena occur in a rather complex yet interesting combination.

2.3 Approach to Mechanics

Given the need to deal with both elastic and time-dependent (dissipative) deformations, it is important to develop approaches that are soundly based on thermodynamic principles. Mechanics is based on the concepts of mass, length and time, from which we derive force and displacement, stress and strain, work and energy, and related quantities. Temperature and heat are added in thermodynamics. The intuitive ideas of a spring and a dashpot are used as a basis, with material degradation over time leading to a change in material properties and to the response of the spring and dashpot to stress. The work of Biot and Schapery as introduced in Part II and Appendix A provides the foundation to the approach, based on the thermodynamics of irreversible processes (TIP). Bridgman (1941) gives very useful perspective on the first law from the operational point of view that he advocates. If one is dealing with a body, and we are considering a bounding surface around the region of interest, one imagines "sentries" posted at points around the boundary, each with instruments capable of measuring the amount of heat passing through their element of the bounding surface, or the flux of mechanical energy by means of measurement of stress and displacements. Much of this can now be studied using numerical and finite element analysis. The flux of mechanical energy into a small volume of material is causative in the microstructural changes to the material, which effectively alter its mechanical properties, especially its time-dependent response.

https://doi.org/10.1017/9781108674454.003 Published online by Cambridge University Press

In large ice masses, such as multiyear ice or icebergs, the ice crystals are found in an irregular array of more or less random arrangements, but fitting together. The process to be analysed leads to breakdown of the original structure by microfracturing and by dynamic recrystallization or by fracture. In processes involving dynamic recrystallization, the ice crystal structure develops a granular, equiaxed morphology. The crystals will initially be of different sizes, and any attempt to follow the fate of individual crystals would quickly lead to an intractable problem, given the objective of studying the full failure process of the ice feature up to and after the occurrence of peak load. Much of the analysis of mechanics in Part II has been conducted using the finite element program ABAQUS and associated user material subroutines UMAT and VUMAT. Ice is in general treated as being statistically isotropic. The condition (state) of particular points in the continuum have been represented by internal state variables. With regard to fracture, the approaches of Barenblatt as extended by Schapery to include time-dependence are the most appropriate for the present work.

A statement of the first law of thermodynamics has been given by Bridgman (1941):

$$\Delta u = \Delta h + \Delta w, \tag{2.1}$$

where Δu = gain of internal energy for the region of interest, Δh = heat received and Δw = work received by the region from its surroundings, during any time interval. For the purposes of the analyses in the present work, entropy S is associated with the generation of heat h in processes including viscoelasticity, sliding of particles, frictional movements and dynamic recrystallization. Grain refinement can lead to substantially increased viscous flow. Entropy change dS is given by

$$dS = \frac{dh}{T}, \tag{2.2}$$

where T is temperature. The unit of entropy is J K^{-1}. There are small differences to be recognized in the elastic properties under isothermal versus adiabatic conditions; these are summarized in Appendix A.

2.4 Creep of Ice

In introducing the creep of ice, we first make a connection to the work of Andrade (1910). He reported on experiments of tensile creep of lead, lead-tin alloys, and copper, and observed that the deformation could be divided into three parts: (i) the immediate extension upon loading; (ii) an initial flow which gradually disappears; and (iii) a constant flow, taking place throughout the extension. It is most useful to distinguish between elastic strain, delayed elastic strain, and flow, as these can be related directly to viscoelastic theory. The strain due to a constant small stress that is applied uniaxially and removed after a period of time is shown in Figure 2.3. We write the strain under constant uniaxial stress as

$$\epsilon = \epsilon_e + \epsilon_d + \epsilon_f, \tag{2.3}$$

https://doi.org/10.1017/9781108674454.003 Published online by Cambridge University Press

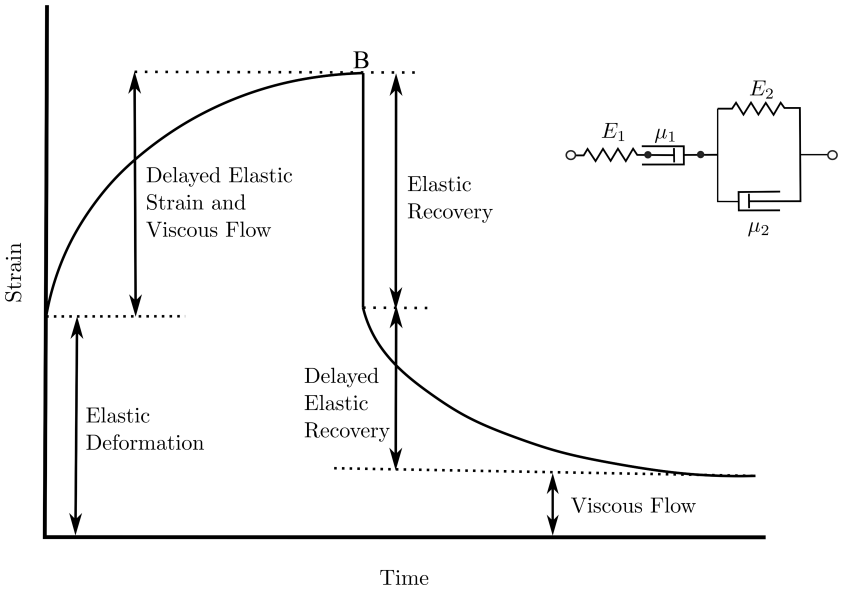

Figure 2.3 Components of creep for low stress. Stress applied at the origin of the time axis and removed at time corresponding to point B shown in figure. The Burgers unit is illustrated.

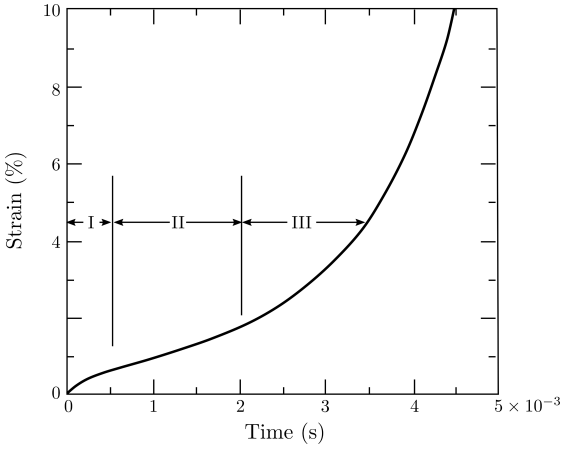

Figure 2.4 The three stages of creep at higher stress levels: primary, secondary and tertiary (after Mellor and Cole, 1982, with permission from Elsevier).

where ϵ_e, ϵ_d and ϵ_f are the elastic, delayed elastic and the flow components of strain. The elastic strain is recovered immediately upon unloading, whereas the delayed elastic component recovers over a period of time. For higher stresses and longer periods of time, there are three approximate stages: primary (I), secondary (II) and tertiary (III), as shown in Figure 2.4. In the last of these stages, the strains accelerate, largely associated with damage processes. Ice does exhibit the minimum creep rate as shown in Figure 2.4, given a high enough level of stress. Conceptually, the deformation of Figure 2.3 can be modelled as a Burgers unit (Figures 2.3 and 6.7)—more on such models

https://doi.org/10.1017/9781108674454.003 Published online by Cambridge University Press

in Chapter 6. The third component of this subdivision ϵ_f we term "flow", irrecoverable viscous strain. In ice there will inevitably be microstructural change except for deformations at very low stresses and for short durations of loading. Elasticity involves largely reversible processes, while the flow term, and dashpots in general, involves dissipation and increases in entropy. The elasticity of the ice crystal is detailed in several references, including the recent work by Schulson and Duval (2009), who also discuss creep deformation of single crystals as well as polycrystalline ice.

We shall adopt the equations of Sinha (1978, 1979), which follow this subdivision of strain. We deal with compressive states so that we take these as being positive, with associated contractive deformations as being positive also. Sinha's work was concerned with low stresses, generally less than 1 MPa, and with uniaxial loading of the specimens. Various temperatures were considered including a base for comparison of response at –10°C. His equation for strain under constant stress reflects the three components of strain as discussed:

$$\epsilon\,(t) = \frac{\sigma}{E}\left\{1 + \frac{c_1 d_1}{d}\left[1 - \exp\,(a_T t)^b\right]\right\} + \dot{\epsilon}_0 t\left(\frac{\sigma}{\sigma_1}\right)^n, \tag{2.4}$$

where σ is the stress, E is the elastic modulus, d is the average grain diameter and c_1, d_1, a_T, b are constants. The term for flow, derived essentially from Glen (1955), contains the constants $\dot{\epsilon}_0, \sigma_1$ and n; Glen found $n \simeq 3$. The latter relationship is Glen's law. For a discussion of equations for creep of ice, see also Ashby and Duval (1985).

The mechanisms involved are associated with movements of dislocations through the crystal lattice, and Sinha postulates grain boundary sliding as the mechanism associated with delayed elastic strain. It is noted in Duval et al. (1983) that non-basal slip requires a stress of at least 60 times that of basal slip at the same strain rate. This anisotropy and resulting distribution of internal stresses were analysed, based largely on experimental observations. The redistribution was interpreted by Duval et al. (1983) as the basis for delayed elastic strain. The relationship between single-crystal behaviour and polycrystalline ice was studied later by Schapery (1993, 1997a) with a focus mainly on S2 ice. The elastic properties were estimated using self-consistent and bounding methods, and the results were extended to viscoelastic analysis using the elastic-viscoelastic analogy (see Section 6.9). The use of viscoelasticity is appropriate and the reaction between the crystals was analysed for basal-plane shearing. This was carried out with a power-law input. The use of activation energy is outlined in Section 2.8.

We can write equation (2.4) as

$$\epsilon\,(t) = \frac{\sigma}{E} + \frac{\sigma}{E_k}\left[1 - \exp\,(a_T t)^b\right] + \frac{\sigma}{\mu\,(\sigma)}, \tag{2.5}$$

where E_k is the modulus for delayed elastic strain, and $\mu\,(\sigma)$ is a stress-dependent viscosity $\propto 1/\sigma^{n-1}$. The two terms describing creep in equation (2.5) are the primary and secondary creep components. It is important to distinguish the linear terms in equations (2.4) and (2.5), as we wish to know whether to use methods of linear viscoelasticity. The elastic modulus E and the coefficient $E_k = (c_1 d_1/d)$ indicate linear elastic and delayed elastic terms, yet a complication is presented by the exponent b

https://doi.org/10.1017/9781108674454.003 Published online by Cambridge University Press

in the equation for the latter. A linear viscoelastic equation for delayed elastic strain would typically correspond to the form $b = 1$. See Chapter 6. Note that for small t,

$$1 - \exp(a_T t)^b \simeq (a_T t)^b. \tag{2.6}$$

This is similar to Andrade's expression for the "flow which gradually disappears", which is written as

$$\beta t^b, \tag{2.7}$$

where t is time and β and b are constants, with $b \simeq 1/3$. He termed this β-flow and acknowledged that it should have a finite limiting value at large times. The expression βt^b does not have such a limit but provides excellent fits over decades of values of strain. It is a linear viscoelastic term with a distinct spectrum (see Section 6.8).

We can therefore conclude that, at least for small time intervals during primary creep, ice may be treated as a linear viscoelastic material. This approximation is valid for about 100 seconds, during which time secondary creep is small or negligible. The primary creep eventually reaches a limit. The rate after this stage corresponds to the "minimum creep rate" of secondary creep, as shown in Figure 2.4. The creep rate then accelerates. Ashby and Duval (1985) analysed a variety of data sets and developed a model for polycrystalline ice that agreed well with data up to the minimum creep rate. Schapery (1991a) re-analysed the data using a model based on the "modified superposition principle" (MSP) which included the effects of damage (microstructural change) and showed that good agreement with data could be achieved, including the accelerating creep rate in tertiary creep. Indeed, it was suggested that the minimum creep rate itself arises from damage processes.

The creep relationship of Sinha as introduced above provides an adequate basis for our discussions, especially as the strain is divided into the three components as observed. This is most useful for our introduction of viscoelasticity in Chapter 6. We emphasize that the states of stress in actual ice–structure events in the field are a far cry from the uniaxial low-stress conditions employed in creep testing. These conditions simply do not extrapolate at all to the actual conditions when ice interacts with a structure.

2.5 Pressure Melting of Ice

The fact that water expands upon freezing leads to the phenomenon of pressure melting: when pressure is applied to ice, the melting temperature reduces. For example, a pressure of about 135 MPa would decrease the melting point to –10°C. One of the earliest applications of thermodynamics was concerned with this subject, going back to Clapeyron and James Thomson. Experimental data on this question were presented by Bridgman (1912). The phenomenon has profound consequences with regard to the behaviour of ice in compression. We first note that when a piece of ice melts, its volume is reduced. As a result, work is done on it by atmospheric pressure. The ice requires the provision of latent heat equal to L per unit mass to melt, and part of this

https://doi.org/10.1017/9781108674454.003 Published online by Cambridge University Press

is provided by the work just noted, i.e. the atmospheric pressure times the change in volume. If the piece of ice at a given temperature, T_0, solid but close to melting, subjected to a lower temperature, it remains solid. But if an additional pressure is applied, for instance by mechanical means, then more work is done by the pressure during melting and less heat needs to be supplied to make up the latent heat. Melting then takes place at a temperature that is lower than the original given temperature T_0. As a result, melting will take place if sufficient pressure is applied; without the additional pressure, melting would not take place.

More formally, we consider a small amount of ice, say 1 g, under hydrostatic pressure p and with latent heat of fusion L. The ice is at its melting point T. As it melts, it contracts by the amount $(v_i - v_w)$, where v is the specific volume and the subscripts i and w refer to ice and water, respectively. The work done on the ice as it melts is

$$p\,(v_i - v_w). \tag{2.8}$$

If a small additional pressure is applied, increasing to the value $p + dp$, there is an additional amount of work on the ice during melting, equal to

$$dp\,(v_i - v_w). \tag{2.9}$$

The entropy change for melting is

$$S = \frac{L}{T}. \tag{2.10}$$

If the melting temperature changes by dT, we can estimate the entropy change from

$$\frac{dS}{dT} = -\frac{L}{T^2}, \text{ and} \tag{2.11}$$

$$TdS = -\frac{L}{T}dT. \tag{2.12}$$

Equating this heat to the additional work,

$$dp\,(v_i - v_w) = -\frac{L}{T}dT, \text{ and} \tag{2.13}$$

$$\frac{dT}{dp} = -\frac{T\,(v_i - v_w)}{L}. \tag{2.14}$$

This can be derived also by considering the Gibbs free energy

$$G = u + pv - TS, \tag{2.15}$$

where u is the internal energy and S, as before, the entropy. At equilibrium, the specific Gibbs free energies of the solid and liquid are equal. When we add heat at constant volume, this becomes

$$-S_i\,dT + v_i\,dp = -S_w\,dT + v_w\,dp, \tag{2.16}$$

https://doi.org/10.1017/9781108674454.003 Published online by Cambridge University Press

and, as a result

$$\frac{dT}{dp} = \frac{v_i - v_w}{S_w - S_i}, \text{or} \tag{2.17}$$

$$\frac{dT}{dp} = -\frac{T\,(v_i - v_w)}{L}, \tag{2.18}$$

as before. Equation (2.18) is the Clausius-Clapeyron relationship. Using equation (2.18), the accepted result for ice at 0°C is a decrease of 0.0738°C MPa^{-1} (Hobbs, 1974).

Bo Nordell (1990) designed an ice-powered cart, the driving force of which was obtained from the pressure-volume work of freezing water. This developed into an interest in pressure melting. He carried out experiments and extended equation (2.18) to take into account the thermal expansion and volume change at constant pressure and constant temperature. He obtained a nonlinear relationship replacing equation (2.18), which agreed well with his experimental results and those of Bridgman and coworkers. The linear relationship of equation (2.18) with the value of 0.0738°C MPa^{-1} gives good results up to 50 MPa, and deviating (underestimating the decrease in temperature) by about 7% at 100 MPa. Although surface pressures up to about 70 MPa have been measured in indentation tests, these values would be the sum of volumetric and deviatoric components. The associated hydrostatic pressures would be of the order of 40 MPa. Nordell's test results show that a confining pressure of about 110 MPa is required to lower the melting temperature to –10°C. The International Association for the Properties of Water and Steam gives refined relationships. It is interesting to note that, with increasing pressure, the melting point decreases to a minimum of about −22°C at 210 MPa. Thereafter, the pressure melting point rises with pressure, passing back through 0°C at 632 MPa.

2.6 Dynamic Recrystallization

Dynamic recrystallization refers to the nucleation and growth of new grains of a material during deformation. The adjective "static" is reserved for recrystallization that is not associated with the deformation. Dynamic recrystallization (DRX) is a softening mechanism in metals and alloys during deformation (under stress) at elevated temperatures. Strong decreases in grain size may lead to diffusive mass transfer (Urai et al., 1986). The area of interest in the present work is the dynamic recrystallization of ice under stress, whereby a strong decrease in grain size does indeed result. In the high-pressure zones (*hpz*s) referred to earlier in Section 2.1, high values of shear stress combine with a range of hydrostatic pressures, from low to high. Results regarding this phenomenon are discussed in many sections of this work, particularly in Section 4.7 on medium scale testing and in Chapter 7 on triaxial testing. The process leads to extensive microfracturing combined with recrystallization at low hydrostatic pressures and extreme grain refinement at high hydrostatic pressures. Thin sections of ice illustrating this process are given in Chapter 7; reference is also made to Melanson et al.

https://doi.org/10.1017/9781108674454.003 Published online by Cambridge University Press

(1999), Meglis et al. (1999) and Jordaan and Barrette (2014). At the centre of the *hpz* during deformation under high shear and pressure, the dominant deformation mechanism is much enhanced flow, certainly nonlinear with stress. An extreme softening process takes place in ice; the effects of pressure melting add to this.

The changes in structure are driven by mechanical processes and the use of free energy (e.g. Cottrell, 1975). This will be principally elastic strain energy; in Jordaan et al. (2005b), the strain energy and dislocation density with associated energy were estimated. Dislocation density is described as leading to dynamic recrystallization in metals, when the metal is raised to the recrystallization temperature. Alaneme and Okotete (2019) reviewed the mechanisms of recrystallization and noted lattice strains and crystalline imperfections as being important, with dislocations being the main contributors. Eshelby (1971) states that the "effective force on crack tip" = J integral = "energy release rate is closely related to the force on a defect (dislocation, impurity atom, lattice vacancy and so forth)". The states of stress vary considerably, being under triaxial compression in a high-pressure zone. No doubt, these states of stress, when superimposed on material containing dislocations, will increase the local stress concentration and energy. Stress concentrations between grains will lead to localized pressure melting. The fine-grained structure and associated strong decrease in grain size lead to a change in deformation mechanism from creep to a process where finely grained particles are extruded, with extremely small pieces of ice moving and mixing with others. The mechanical behaviour of the microstructurally modified ice has been measured in a series of experiments using a triaxial cell (Section 7.4).

With regard to the geophysical analogue of this process, mylonite formation is discussed in Urai et al. (1986). Etheridge and Wilkie (1979) suggested that dynamic recrystallization alone is insufficient to cause enough weakening to result in flow of mylonites. This is certainly not the case for ice, in which deformation is also aided by pressure melting. Whether this is a factor in any mineral deformation is a subject for consideration. Very high pressures and temperatures do exist in mylonite formation; Garlick and Gromet (2004) state that diffusion creep does occur with partial melting in the formation of high temperature mylonitic gneisses. These few words are not intended to be a survey of literature; the purpose is to point out the analogy between the processes in ice under compressive stress and those in mylonite formation (at vastly different scales).

2.7 Microstructurally Modified Ice: Development of Layers

The "layer" of ice, a seemingly minor detail of compressive ice–structure interaction, turns out to be highly significant in understanding compressive ice failure. Under compression, especially those non-uniform states that occur in interaction with structures or under indentation, ice is prone to develop zones with microstructurally modified texture, and particularly zones of recrystallized ice. We introduce these generally in this section (see also Jordaan et al., 2009) with regard to past experiments, and return to the subject in discussing medium scale indentation in more detail (Section 4.6).

https://doi.org/10.1017/9781108674454.003 Published online by Cambridge University Press

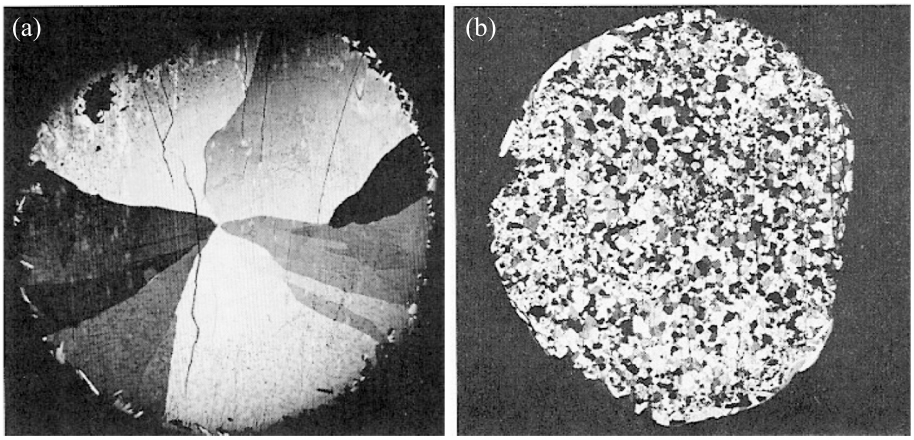

Figure 2.5 (a) Original grain structure of ice specimens of bubble free ice. (b) microstructure of bubble-free ice extruded at a strain rate of 5.6×10^{-2} s^{-1} at a temperature of –20.5°C. From Kuon and Jonas (1973). This content has been reproduced with the permission of the Royal Society of Canada.

Barnes et al. (1971) studied the friction on a cone of single-crystal ice sliding over a hard surface. They observed recrystallization to occur at the interface. The formation of this zone of recrystallized ice helped account for the increased rate of creep found in the friction experiments versus comparable compression experiments. Offenbacher et al. (1973) studied recrystallization of single crystals of ice using thin ice specimens and a transparent glass surface, which could be moved at speeds ranging from 0.05 to 4 mm s^{-1}. By observing the contact zone between the ice and glass plate, it was noted that at loads above about 1.5 kg (or at lower loads that were held for longer periods of time), "permanent changes occurred immediately", with diameter of the recrystallized area about 2 mm. Cracks were often produced in a direction perpendicular to the c-axis. Recrystallization was found to begin along these cracks and then spread into the deformed region of the ice. The inadvertent presence of a grain boundary caused similar recrystallization behaviour to occur.

Kuon and Jonas (1973) performed tests aimed at studying the effects of strain rate and temperature on the extrusion behaviour of ice. These authors tested samples of ice with and without air bubbles. The test specimens were 4.12 cm in diameter and 20 cm in length. The bubble-free specimens consisted of large columnar grains extending from the outside to the centre of the sample. In the case of the ice containing bubbles, the ice had a columnar structure over most of the sample with a central core containing equiaxed grains. Tests were performed by extruding the specimens of ice through a die and hollow ram. It was found that at constant extrusion temperature, the grain size decreased with increasing strain rate. At constant strain rate on the other hand, the grain size increased with temperature. In all cases, considerable reduction in grain size occurred; Figure 2.5 shows one result. The authors speculated that subgrains observed within some of the recrystallized grains were formed during the deformation and consequently were caused by dynamic recrystallization. Frederking and Gold

https://doi.org/10.1017/9781108674454.003 Published online by Cambridge University Press

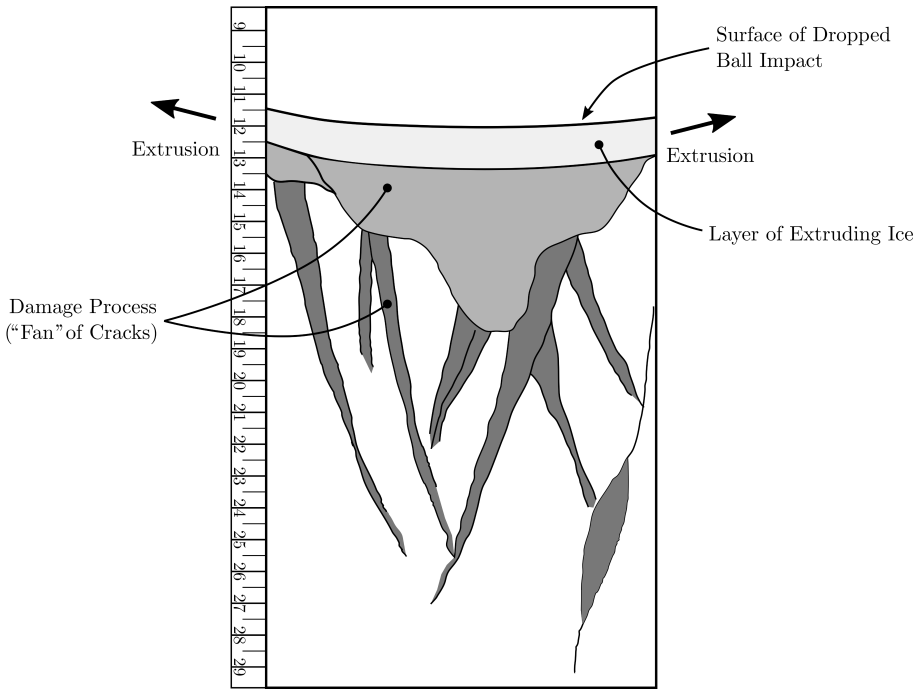

Figure 2.6 Writer's representation of ice section after dropped-ball test by Kheisin and co-workers. See also original paper by Kheisin and Cherepanov (1970).

(1975) observed a reduction in grain size in regions of high shear during laboratory experiments on indentation of ice plates within the range of ductile behaviour, i.e. at slow rates of interaction.

At high rates of indentation or interaction, a distinct layer of microstructurally modified ice is found. Kheisin and his co-workers (Kheisin and Cherepanov, 1970; Kurdyumov and Kheisin, 1976) described tests conducted in 1967 using a steel ball weighing 300 kg dropped onto the ice surface (freshwater ice of Lake Ladoga). They examined the microstructure before and after the impact. Velocities were in the range 1 to 6 m s^{-1}. They drew attention to the fine-grained nature of the ice in a layer, which covered the entire contact zone. The main features of the results are illustrated in Figure 2.6. The distinct layer is the feature that was exploited in further analysis, and they also noted "fans" of cracks further into the ice. Kheisin and co-workers described the changes to the microstructure in some detail and pointed out that "lamellae up to 0.5 mm thick, formed by shear over the basal planes" were produced. They also pointed to the existence of "ice particles of submicroscopic size dispersed amidst these crystals and acting as a lubricant for the matrix", resulting in a "finely dispersed crushed layer behaving as a layer of viscous liquid". The effect of pressure melting and frictional heating was also described.

In the present work, considerable attention is paid to medium and small scale testing, in which the state of the ice could be examined after testing. Layers of microstructurally modified ice were invariably found, except at very low indentation

https://doi.org/10.1017/9781108674454.003 Published online by Cambridge University Press

speeds. We shall return to discussion of the medium scale tests in Section 4.7 and the small scale tests in Section 8.6. A most important fact that emerges is that the behaviour of ice in these crushed layer is quite different from that of the parent ice. Extrusion of ice particles on a significant scale is a feature of this failure mode, an aspect that is hard to reconcile with conventional mechanics. Time-dependent effects and changes to structure requiring viscoelasticity and damage mechanics are dominant. In the case of the layer, as studied by Kheisin and his colleagues, it was treated as being viscous, distinct in properties from the parent ice. This acknowledgement of reality was a big step forward in ice mechanics, as the distinction between the properties of ice in an unmodified state, on the one hand, and ice that is microstructurally modified and under high compression, on the other hand, is really important to the understanding of how ice fails in compression. The approach taken by Kheisin and co-workers was to treat the layer as a linearly viscous material with its own viscosity. This approach is described in outline form in Section 6.4.

2.8 Thermally Activated Processes

Many processes can be modelled as being thermally activated: movements of dislocations in metals and other materials, structural changes including recrystallization and fracture processes are examples (Krausz and Eyring, 1975). We can certainly conceive of creep movements as being thermally activated. The material is in equilibrium which is disturbed by repeated thermally activated events. A particle that acquires an energy equal to or greater than the activation energy e_A is able to surmount an energy barrier and move into a position of lower potential energy (Cottrell, 1964, 1975). These movements are observed macroscopically as creep of the specimen.

We consider a particle oscillating about a certain mean position. Let E be the event of a particle surmounting the energy barrier e_A in a "run" at the barrier. Noting that the energy level $e_i = ih\nu$, where h = Planck's constant, ν = frequency, and $i = 1, 2, 3,....$, the classical Maxwell-Boltzmann distribution of energy amongst particles (summarized in Jordaan, 2005) is expressed as follows:

$$p_i = \frac{\exp\left(-e_i/kT\right)}{\sum_j \exp\left(-e_j/kT\right)}. \tag{2.19}$$

Then the probability of event E is given by

$$\Pr\left(E\right) = \frac{\sum_{e_i > e_A} \exp\left(-e_i/kT\right)}{\sum_j \exp\left(-e_j/kT\right)} \tag{2.20}$$

$$= \frac{\sum_i \exp\left[-\left(e_A + ih\nu\right)/kT\right]}{\sum_j \exp\left(-jh\nu/kT\right)} \tag{2.21}$$

$$= \frac{\exp - \left(e_A/kT\right) \sum_i \exp\left[-\left(ih\nu\right)/kT\right]}{\sum_j \exp\left(-jh\nu/kT\right)} \tag{2.22}$$

$$= \exp\left(-\frac{\epsilon_A}{kT}\right). \tag{2.23}$$

https://doi.org/10.1017/9781108674454.003 Published online by Cambridge University Press

If ν = the number of runs per second at the barrier, the rate of a spontaneous reaction using the theory of activation energy is

$$\nu \exp\left(-\frac{\epsilon_A}{kT}\right). \tag{2.24}$$

This may be written as a frequency f per second

$$f = \nu \exp\left(-\frac{Q}{RT}\right), \tag{2.25}$$

where Q is the activation energy per mole of particles and R is the gas constant. This may also written as strain rate:

$$\dot{\epsilon} = A \exp\left(-\frac{Q}{RT}\right), \tag{2.26}$$

see for example Glen (1955). The term A is called the "pre-exponential factor".

This relationship has been used extensively in the literature on creep of ice, for example Barnes et al. (1971), Glen (1955) and Sinha (1978). One can plot $\log \dot{\epsilon}$ against the reciprocal of absolute temperature to test the relationship and to use it to making inferences regarding the value of Q. This was done by Barrette and Jordaan (2003) for the minimum creep rate under various triaxial loadings. This is discussed in Section 7.5. Schapery (1996, 1997b) included discussion of molecular models in nonlinear viscoelastic analysis.

2.9 Fracture Processes

Fractures are omnipresent in ice mechanics. Gold (1963) recognized the importance of the extreme brittleness of ice. Palmer et al. (1983) correctly emphasized the role of fracture in estimating ice forces. There have been several good test programmes of measurement of fracture toughness. Yet there has been little progress in development of analytical tools based directly on fracture mechanics for use in engineering design. To take the most prominent example of the effect of fracture, we consider compressive "crushing" failure. We know from measurements that the load transmitted to the structure is concentrated in a small percentage, of the order of 10%, of the area defined by the global area, obtained from the original unfractured profile of the ice. The load becomes localized into many high-pressure zones (*hpz*s), as illustrated in Figures 2.1 and 2.2. Design methods are generally based on an empirical analysis of measured pressures. A method that is defensible on a probabilistic basis is one in which *hpz*s are modelled as a random set of loads at spacing that is partly random (e.g. spaced randomly but near the centre of ice sheets). This is described in Section 3.4 for the case of ships ramming thick ice. Fracture mechanics has not fully explained the very important spalling events that cause the localization and the resulting 10% of global area that constitutes the loaded area.

https://doi.org/10.1017/9781108674454.003 Published online by Cambridge University Press

A further complication is that, as with other aspects of ice deformation, fracture is time-dependent, with viscoelastic movements highly involved in the fracture process. Strong evidence in the field was found during the medium scale testing that slow indentation results in a permanent "dent" in the ice with little or no spalling, whereas for faster loading a considerable amount of spalling occurred with *hpz* formation. Yet slower loading of longer duration can lead to sudden large fractures; this is described in Section 4.7. Icebreaker captains have reported that "leaning on the ice" can lead to time-dependent fracture of an ice floe. Large floes have been observed to split into pieces after a period under load (Figure 4.8). Reference is made to Chapter 9 for an analysis of time-dependency. As a result it is difficult to use the notion of "ductile to brittle transition" which has been borrowed from study of the behaviour of metals with regard to temperature. In ice mechanics "transition" is used with regard to strain or loading rate. In reality ice behaviour is more of a continuum. There is a transition to layer formation and extrusion from more widespread damage formation. Even in uniaxial testing, macroscopically "ductile" behaviour can result from a distribution of microcracks.

The theoretical strength of a material can be calculated as the stress required to break atomic bonds, and calculations show this to be of the order of $E/10$, where E is the elastic modulus. In the case of ice, this would give values of the order of 900 MPa, much greater than the tensile strength of ice, which is of the order of 1 MPa. As is well known, the difference is related to flaws, irregularities and defects in the material. The flaw that is studied in fracture mechanics is generally the crack. Depending on the state of stress in the material, the crack can be subjected to tensile stress, resulting in the "opening mode" of crack separation, or to shearing stresses, resulting in the "sliding" and "tearing" modes. We shall focus on the opening mode in the present work. To motivate an approach to fracture, we can think conceptually of a body with a crack of length $2a$, a being the half-length, with a tensile stress applied. Then the failure stress σ_f is related to crack length by the following:

$$\sigma_f \propto K_c / \sqrt{a}, \tag{2.27}$$

where K_c is the fracture toughness, a material constant. The longer the crack, the smaller the failure stress, which accords with common experience. Approximate values of fracture toughness of various materials (in kPa $\sqrt{\text{m}}$) are as follows: steel, 50,000; stainless steel, 200,000; aluminium, 20,000; ceramic, 4,000; soda lime glass, 750; and PMMA, 1,000. Timco and Frederking (1986) performed early measurements on ice in which fracture toughness values of the order of 100–140 kPa $\sqrt{\text{m}}$ were reported, very small values compared to other materials. The resulting energy release rate, taking the elastic modulus as 10 GPa, is in the range 1–2 J m^{-2}. Results on fracture toughness are reviewed in more detail in Chapter 9.

Events such as floe splitting (Figure 4.8) have received some attention with regard to load estimation but it is difficult to include these events in design calculations given present knowledge. It is important to study such events in future work using fracture mechanics, especially fractures induced in icebreaking. In the case of a large ice feature, such as a multiyear ice floe interacting with a structure, the large fractures

https://doi.org/10.1017/9781108674454.003 Published online by Cambridge University Press

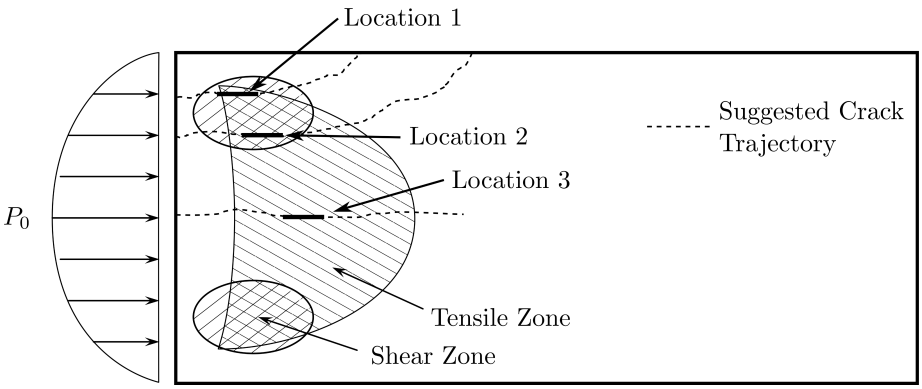

Figure 2.7 Possible fracture and spall zones shown in vertical section of beam under load (from Zou et al., 1996, with permission from Elsevier).

might relieve load (but likely not immediately); to put this into a probabilistic design context with appropriate mechanics, one has to know what is the probability of the fracture happening, where it might happen, and what stress relief results. The stress relief might be quite small in the case of a wide structure. While the fracture of large ice features is certainly of interest, other fracture events deserve attention, especially those involved in the formation of high-pressure zones.

It seems clear that the fractures associated with the formation of *hpz*s are relatively small—not of the size exhibited in floe splitting, or in fracture of large floes in icebreaking—but rather of the order of 1 or 2 metres, more or less. With regard to the formation of spall fractures and consequent localization, some studies have been initiated. Matskevitch and Jordaan (1996) related the confinement and state of stress that occurs in *hpz*s to the outwardly sloping sides observed in *hpz* formation. This has been illustrated in a general way in Figure 2.1. The sources of crack initiation in a stressed beam were explored by Zou et al. (1996), and the results are illustrated in Figure 2.7. Dempsey et al. (2001) considered the *hpz* as a hollow cylinder with pressure applied internally and externally. Pressure within the hollow cylinder is applied to the material, and the authors studied crack propagation from the inner cylinder, a very idealized situation. Taylor and Jordaan (2015) conducted a detailed investigation, the basis of which is illustrated in Figure 2.8. A spatial density of cracks was considered, based on grain size (Cole, 1986), with a random orientation. A simulation procedure was followed, whereby cracks were modelled and investigated as to their propensity to propagate. Figure 2.8 shows the initiating flaw and the stress field. This was carefully studied for various locations of crack appearance. Using LEFM, a wide range of situations were modelled: sheet ice of various thickness, tapering edges and eccentricity of loading. The results are promising and should form a good basis for further research. It is noteworthy that a scale effect with regard to thickness was found, following $(\text{thickness})^{-0.50}$.

The localization into *hpz*s is in engineering practice handled empirically by using measured data to estimate local and global design pressures, as described in Chapters 3–5. Treating *hpz*s as random localized loads with random spacing can capture well

https://doi.org/10.1017/9781108674454.003 Published online by Cambridge University Press

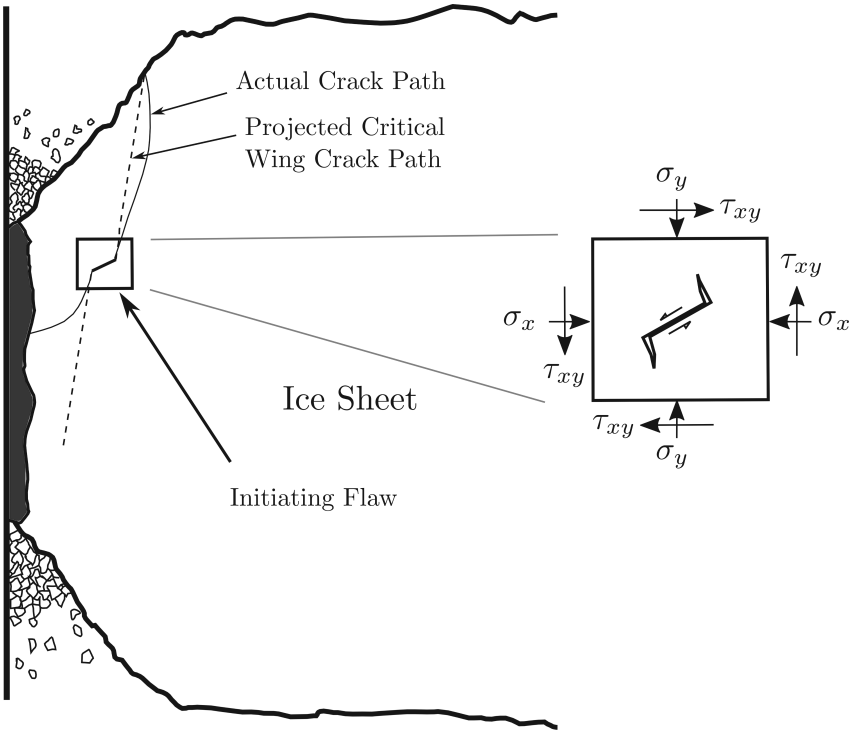

Figure 2.8 Schematic of analysis by Taylor and Jordaan (2015), with permission from Elsevier.

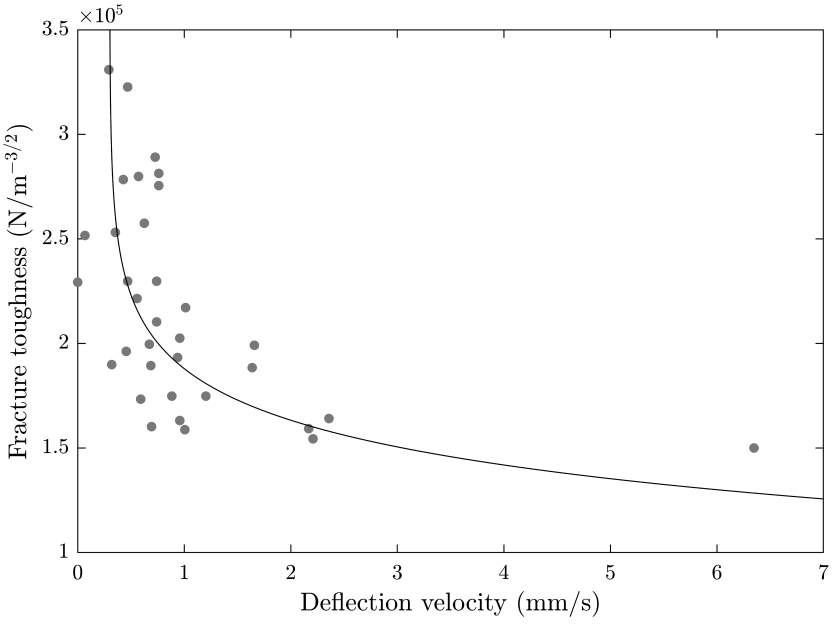

Figure 2.9 Variation of apparent fracture toughness with rate of displacement in four-point bending test on ice samples (Kavanagh et al., 2015) with power-law fit. With permission from ASME.

https://doi.org/10.1017/9781108674454.003 Published online by Cambridge University Press

the observed behaviour and distribution of pressure for design purposes. The spacing should reflect the geometry of the interaction; for thin sheets for example, the loading is oriented along a line near the centre, the well-known line-like loading (Section 4.2).

Fracture is discussed in more detail with emphasis on time-dependent effects in Chapter 9. To illustrate the importance of time, Figure 2.9 from Kavanagh et al. (2015) shows an almost 3-fold variation of apparent fracture toughness. Care must be taken to understand time-dependent effects in ice fracture generally and in particular in postulating a scale effect of fracture toughness. The early work on cracks concentrated attention on the elastic stresses at crack tips, which were analysed as infinite, associated with a singularity. This was overcome partly by Griffith who considered the energy transferred in crack extension rather than crack tip stresses, and by Barenblatt, who eliminated the crack-tip singularity, using linear elastic theory. This was taken up by Schapery to study time-dependent effects and nonlinearity. These matters are considered to be research topics, and are deferred to Chapter 9 in Part II of this book.

https://doi.org/10.1017/9781108674454.003 Published online by Cambridge University Press